Proton Transfer Dynamics at the Membrane/Water Interface: Dependence on the Fixed and Mobile pH Buffers, on the Size and Form of Membrane Particles, and on the Interfacial Potential Barrier

Dmitry A. Cherepanov,*† Wolfgang Junge,* and Armen Y. Mulkidjanian*‡
*Division of Biophysics, Faculty of Biology/Chemistry, University of Osnabrück, D-49069 Osnabrück, Germany; †A. N. Frumkin Institute of Electrochemistry, Russian Academy of Sciences, 117071 Moscow, Russia; and ‡A. N. Belozersky Institute of Physico-Chemical Biology, Moscow State University, Moscow, 119899, Russia

ABSTRACT Crossing the membrane/water interface is an indispensable step in the transmembrane proton transfer. Elsewhere we have shown that the low dielectric permittivity of the surface water gives rise to a potential barrier for ions, so that the surface pH can deviate from that in the bulk water at steady operation of proton pumps. Here we addressed the retardation in the pulsed proton transfer across the interface as observed when light-triggered membrane proton pumps ejected or captured protons. By solving the system of diffusion equations we analyzed how the proton relaxation depends on the concentration of mobile pH buffers, on the surface buffer capacity, on the form and size of membrane particles, and on the height of the potential barrier. The fit of experimental data on proton relaxation in chromatophore vesicles from phototropic bacteria and in bacteriorhodopsin-containing membranes yielded estimates for the interfacial potential barrier for H^+/OH^- ions of ~120 meV. We analyzed published data on the acceleration of proton equilibration by anionic pH buffers and found that the height of the interfacial barrier correlated with their electric charge ranging from 90 to 120 meV for the singly charged species to >360 meV for the tetra-charged pyranine.

INTRODUCTION

The transmembrane difference in electrochemical potential of hydrogen ion ($\Delta\tilde{\mu}_{H^+}$) plays a key role in biological energy transduction. This difference is generated by redox- or light-driven proton pumps in the energy-transducing membranes of bacteria, chloroplasts, and mitochondria. After Mitchell (1961), the protonmotive force (*pmf*) is written as

$$pmf = \Delta\tilde{\mu}_{H^+}/F = \Delta\psi - 2.3RT/F\times\Delta pH, \quad (1)$$

where $\Delta\psi$ is the transmembrane electric potential difference and ΔpH is the transmembrane pH difference.

In bacteria, protons are extruded by pumps out of the cell. Without constraints on proton diffusion, as first noted by Williams, the ejected protons would be diluted in the infinite external solution and the entropic component of *pmf* would be lost; see, e.g., Williams (1978) and references therein. This argument is crucial for alkaliphilic bacteria, such as *Bacillus firmus*, which clamp their internal pH by ~3 pH units more acidic than the ambient one (see Krulwich et al. (1996) for a review). As $\Delta\psi$ in these bacteria hardly increases above 200 mV (Guffanti et al., 1984), the application of Eq. 1 yields a *pmf* value of about zero. A wealth of data obtained with other bacteria revealed a poor correlation between the magnitude of *pmf*, which was calculated as the sum of ΔpH (between two water phases) and $\Delta\psi$, and the efficiency of various *pmf* consumers, the ATP synthase in the first line (see, e.g., Michel and Oesterhelt (1980) and Elferink et al. (1983) for original data and Kell (1979), Ferguson (1985), and Cramer and Knaff (1991) for the surveys). To account for these kinds of observations, Kell (1979) hypothesized that the ejected protons spread at the membrane surface but were somehow hindered from the prompt equilibration with the bulk. Michel and Oesterhelt (1980) came to the same conclusion based on the poor correlation between the adenosine tri-phosphate (ATP) yield as measured in whole cells of halobacteria and the magnitude of *pmf*, defined as a sum of $\Delta\psi$ and ΔpH. If proton exchange is retarded, the local pH at the membrane surface might differ from the pH in the bulk at steady state, leading to reasonably large values of *pmf* even in the case of alkaliphilic bacteria (see also discussion in Guffanti and Krulwich (1984)).

In the previous work we argued that the diffusion of charged molecules across the membrane/water interface might be restricted by the low dielectric permittivity (ε) of water at negatively charged membrane surface (Cherepanov et al., 2003). Using the permittivity profile as obtained by the atomic force microscopy at the negatively charged mica surface at low (≤1 mM) ionic strength (Teschke et al., 2001), we extrapolated the dielectric properties to the higher ionic strength of ~0.1 M and calculated the potential energy profile for probe ions at the membrane/water interface. We found that the decreased dielectric permittivity of the surface water gave rise to a potential barrier that peaked ~0.5–1 nm away from the surface. The height of barrier depended on the charge and the size of probe ions. It was on the order of 100–200 meV for monovalent spherical ions with radius of 0.25 nm, being higher for anions than for cations. At steady

Submitted July 29, 2003, and accepted for publication September 26, 2003.

We dedicate this article to the memory of Andrey Kaulen, a fine colleague and outstanding scientist.

Address reprint requests to Armen Y. Mulkidjanian, Abteilung Biophysik, Fachbereich Biologie/Chemie, Universität Osnabrück, D-49069 Osnabrück, Germany. Tel.: +49-0541-9692871; Fax: +49-0541-9692870; E-mail: mulkidjanian@biologie.uni-osnabrueck.de.

0006-3495/04/02/665/16 $2.00

operation of proton pumps, such a barrier could raise up the proton concentration at the membrane surface by 10^{-6} M over the value in the bulk. This finding might explain how alkaliphilic bacteria synthesize ATP at the expense of the surface-to-surface *pmf*.

A question might arise to what extent the smooth mica surface can represent the irregular interface of biological membranes. Here we scrutinized the properties of interfacial water at the surface of biological membranes by the quantitative analysis of a variety of experimental data on the proton transfer dynamics as obtained in pulse experiments at moderate ionic strength close to the physiological conditions. In experiments of this kind, the equilibrium was perturbed by a rapid ejection (uptake) of protons at the membrane surface, with the subsequent proton relaxation being monitored by different techniques. The surface/bulk proton relaxation in different membrane preparations and membrane enzymes was found to be substantially slower than the proton equilibration at the surface proper. The relatively fast rate of lateral proton equilibration along the membrane surface is apparently due to the high density of pH-buffering groups at the membrane surface (see Georgievskii et al. (2002), Zhang and Unwin (2002), and Serowy et al. (2003) for the recent quantitative analysis of this issue and relevant references). Several teams have shown independently that hydrophilic pH indicators, when added to a suspension of unsealed bacteriorhodopsin (BR) membranes, picked the BR-ejected protons at ~1 ms, by order of magnitude slower than they arrived and equilibrated at the surface (Drachev et al., 1984, 1992; Heberle and Dencher, 1992; Heberle et al., 1994; Alexiev et al., 1995; Dioumaev et al., 1998; Porschke, 2002). Analogously, it has been shown that protons appeared at the surface of the cells and spheroplasts of purple phototrophic bacteria *Rhodobacter sphaeroides* and *Rhodobacter capsulatus* at $\tau < 5$ ms as followed by electrochromic shift of carotenoid pigments (which correlate with the absorbance changes of an amphiphilic, membrane-bound pH indicator neutral red (Mulkidjanian and Junge, 1994)) but were sensed in the bulk phase by hydrophilic pH indicators only at 30–70 ms (Arata et al., 1987; Jones and Jackson, 1989, 1990). A retardation has been also shown for the proton uptake: i), by the photosystem II of green plants (Haumann and Junge, 1994b), and ii), by the photosynthetic reaction centers (RC) of *Rb. sphaeroides* (Maroti and Wraight, 1997; Gopta et al., 1999).

The slow rate of proton transfer between the surface of biological membranes and the bulk water phase has been commonly attributed to the damping effect of fixed pH buffer at the surface (Junge and Polle, 1986; Junge and McLaughlin, 1987; Jones and Jackson, 1989). However, if the surface pH buffers were alone responsible for the retardation, the rate of proton equilibration had to depend on the concentration of mobile pH buffers or pH indicators (see discussion by Junge and McLaughlin (1987), Gopta et al. (1999), and Georgievskii et al. (2002)). Such a dependence was indeed observed with the pH indicator *p*-nitrophenol added to BR membranes (Drachev et al., 1984). Contrastingly, the response time of another hydrophilic pH indicator pyranine, which was added to the similar BR membranes, remained independent of its concentration in the range of 10–150 μM (Heberle, 1991; Porschke, 2002).

These apparently contradictory observations could be rationalized if one takes into account that the height of the above-noted potential barrier in the interfacial water layer depends on the charge of penetrating ion (Cherepanov et al., 2003). Because the charge of pyranine in the deprotonated state is -4 and the charge of *p*-nitrophenol is -1, one expects a much higher barrier in the former case, in agreement with the experimental observations. Qualitatively it looks like the retardation of proton transfer in pulse experiments resulted both from the damping effect of the surface pH buffers and from the influence of the dielectric barrier.

Aiming at a quantitative analysis of the above-cited kinetic data on proton relaxation at the biological interfaces, we modeled here, by numeric integration of the diffusion equations, the proton equilibration between membrane particles of various form and the surrounding bulk solution. In our previous modeling (Cherepanov et al., 2003), we considered only the mobile proton carriers, but neglected the fixed buffers at the membrane surface because the latter do not affect the proton flux at steady state. In the case of pulse experiments, the participation of fixed pH buffers at the membrane surface cannot be neglected (Junge and Polle, 1986; Junge and McLaughlin, 1987). Therefore here we treated the dependence of proton relaxation on the surface buffer capacity explicitly. Besides this, we analyzed the dependence on the concentration of mobile buffer, on the form and the size of membrane particles, and on the height of the interfacial potential barrier. The comparison of model results with published experimental data allowed to obtain a consistent picture where differences in the ability of various mobile pH buffers to accelerate the proton equilibration between the surface and the bulk water were explained by the difference in their electric charge. The latter largely determined the energy barrier as seen by these buffers. The estimated barrier height varied between 90 meV for the singly charged *p*-nitrophenol and >360 meV for pyranine, which carries four negative charges in the deprotonated state.

RESULTS AND DISCUSSION

Proton transfer dynamics at the outer surface of spherical vesicles

As a starting point, we considered the proton equilibration between the membrane surface and the bulk buffer solution in the absence of any barrier at the surface, i.e., under the assumption that the dielectric properties of water at the interface do not differ from those in the bulk phase. This

assumption corresponds to the discontinuous model of the membrane/water interface, where the membrane phase with the dielectric constant $\varepsilon \approx 4$ borders abruptly the bulk water phase with $\varepsilon \approx 78$, as commonly used when modeling interfacial and membrane phenomena (see, e.g., Israelachvili (1992)). To simplify the calculations, we considered spherical vesicles of radius R surrounded by an infinite bulk solution ($R < r < \infty$). The solvent in a typical experiment contains several mobile acids and bases (pH buffers, pH indicators, neutral water, H_3O^+, and OH^-), which interact by bimolecular collision with each other and with fixed pH buffers at the membrane surface. The latter are believed to be coupled to each other by water molecules forming a proton-conducting continuum, which allows fast proton transfer along the surface (see Georgievskii et al. (2002), Serowy et al. (2003), and references therein). For simplicity, we considered only one species of a fixed buffer, B, at the surface of membrane and a single species of a mobile buffer, C, in the bulk solution, with pK values determined by the respective equilibrium dissociation constants K_B and K_C: $pK_B = -\lg K_B$ and $pK_C = -\lg K_C$.

Let us assume that a short light impulse triggers the rapid turnover of proton pumps and perturbs the preexisting proton equilibrium at the membrane surface in 100 μs, a typical time of proton equilibration at the surface of biological membranes. Let σ_B be the density of fixed buffer at the membrane surface (mol m^{-2}), K_B be the dissociation constant of this buffer (mol m^{-3}). The density of the protonated form of the surface buffer σ_{BH} is therefore

$$\sigma_{BH} = \sigma_B \frac{[H^+]}{[H^+] + K_B}, \tag{2}$$

where $[H^+]$ is the equilibrium concentration of free proton (mol m^{-3}) near the surface (in the absence of surface potential $[H^+]$ is equal to the bulk concentration of proton).

Let $\Delta\sigma_H$ be the surface density of ejected protons (mol m^{-2}), which is equal to the density of operating proton pumps if they turn over only once. After the fast equilibration of ejected protons with the buffer B at the surface, which precedes the ultimate equilibration with the bulk solution, the local equilibrium at the membrane surface can be written as

$$\sigma_{BH} + \Delta\sigma_{BH} = \sigma_B \frac{[H^+] + \Delta[H^+]}{[H^+] + \Delta[H^+] + K_B} \approx \sigma_B \frac{[H^+]}{[H^+] + K_B} + \sigma_B \frac{K_B}{([H^+] + K_B)^2} \times \Delta[H^+], \tag{3}$$

where $\Delta\sigma_{BH}$ is the change in the density of the protonated form of the surface buffer, and $\Delta[H^+]$ is the change in the local concentration of free proton in the vicinity of the interface. In the experiments considered below, the local capacity of fixed buffer at the surface (the effective volume concentration has order of 0.1 M) greatly exceeds the capacity of mobile buffers (the maximal used concentration of the latter was 1 mM). In such a case, almost all ejected protons would reside at the surface buffer, so $\Delta\sigma_{BH} \approx \Delta\sigma_H$. Combining Eqs. 2 and 3, one gets the relation between the number of ejected protons and the change in the local concentration of free proton near the surface:

$$\Delta[H^+] \times \frac{K_B \sigma_B}{([H^+] + K_B)^2} = \Delta\sigma_H. \tag{4}$$

If the concentration of mobile buffer C_0 greatly exceeds the concentration of free protons (the usual condition in biological experiments), the change in concentration of the protonated form of mobile buffer at the surface is

$$\Delta[CH] = \frac{K_C}{K_B} \times \left(\frac{[H^+] + K_B}{[H^+] + K_C}\right)^2 \frac{C_0 \Delta\sigma_H}{\sigma_B}.$$

In the following we assume that pK values of mobile and surface buffers match so that the latter relation simplifies to:

$$\Delta[CH] = \frac{C_0 \Delta\sigma_H}{\sigma_B}. \tag{5}$$

The rate of equilibration for a spherical vesicle of radius R in infinite solution can be calculated by the steady-state flux assuming a constant concentration of diffusing species at the surface (see e.g. Berry et al. (1980); the accuracy of such approximation is discussed below after comparison with the respective numerical solution). The steady-state concentration around the vesicle, $c(r)$, can be then written as

$$c(r) = \Delta[CH] \frac{R}{r},$$

and the total steady-state flux across a surface of radius r is

$$J = -4\pi r^2 D \times dc/dr = 4\pi DR \times \Delta[CH].$$

The rate of relaxation therefore reads

$$\tau^{-1} = \frac{J}{4\pi R^2 \times \Delta\sigma_H} = \frac{DC_0}{R\sigma_B}.$$

This equation can be generalized for the case when several different fixed buffers are present at the membrane surface. If σ_0 is the total surface buffer capacity and the solution contains N mobile buffers ($i = 1 \ldots N$) with the respective buffer capacities $\beta_i = (2.3 \times [B_i] \times [H^+] \times K_i)/(4([H^+] + K_i)^2)$ and diffusion coefficients D_i, the relaxation rate constant reads

$$\tau^{-1} = \frac{\sum D_i \beta_i + 2.3(D_H[H^+] + D_{OH}[OH^-])}{R \times \sigma_0}. \tag{6}$$

Here we treated explicitly the diffusion of H^+ and OH^- (the neutral water is present in great excess, so its diffusion does not limit the total flux).

According to Eq. 6, the rate of proton relaxation around a spherical vesicle is proportional to the weighted sum of the concentrations of all mobile species (including H^+ and OH^-) times their respective diffusion coefficients, and it is

reciprocal to the surface buffer capacity and to the radius of vesicles. Equation 6 states that the proton relaxation is accelerated by mobile pH buffers but slows down with the increase of: i), the surface buffer capacity, and ii), the geometrical size of vesicles. The dependence of the proton equilibration rate on the concentration of mobile and fixed buffers has been discussed previously (Junge and Polle, 1986; Junge and McLaughlin, 1987; Jones and Jackson, 1989; Gopta et al., 1999; Georgievskii et al., 2002). The dependence of proton relaxation on the size of membrane particles vesicles has not been noted so far.

Published data on proton relaxation in various membrane preparations are summarized in Table 1. On one hand, these data corroborate the notion that the proton relaxation time increases with the geometrical size of membrane particles (see also below). On the other hand, the model predicts a rather straightforward dependence of the proton relaxation on the concentration of mobile pH buffers/indicators. Indeed, because the diffusion coefficient of common buffers is one order of magnitude smaller than that of H^+ and OH^-, one could expect that a mobile pH buffer added to a buffer-free suspending medium would accelerate the proton equilibration when its concentration exceeds the concentration of predominant proton carrier (H^+ or OH^-, depending on pH) by one order of magnitude. At neutral pH the ''threshold'' concentration of mobile pH buffer is then expected to be on the order of $\leq 5 \times 10^{-6}$ M. As already noted in Introduction (see also below), the observed ''threshold'' concentrations, at which pH buffers started to accelerate pH relaxation, were often much higher and correlated with the electric net charge of buffer molecules. This behavior cannot be described by Eq. 6.

Thus, the dynamics of proton equilibration across the membrane/water interface cannot be understood without taking into account the effect of an interfacial potential barrier, the height of which is expected to depend on the charge of the penetrating ion. A kinetic model, which includes such a barrier, is described in the following section.

Proton relaxation in the presence of a potential barrier: comprehensive model of interfacial proton transfer

We developed a detailed model of proton transfer dynamics at the membrane/water interface to analyze the experimental data quantitatively. On modeling we considered the protolytic interactions and diffusion of four chemical species: 1), a fixed pH buffer at the membrane surface *B*; 2), a soluble pH buffer (pH dye) in the bulk phase *C*; 3), the hydrated proton H^+; and 4), the hydroxyl anion OH^-. The protolytic interactions in the system were described by the following reactions:

$$B^- + H^+ \underset{k_{2B}}{\overset{k_1}{\rightleftharpoons}} BH$$

$$C^- + H^+ \underset{k_{2C}}{\overset{k_1}{\rightleftharpoons}} CH$$

$$BH + OH^- \underset{k_{4B}}{\overset{k_3}{\rightleftharpoons}} B^-$$

$$CH + OH^- \underset{k_{4C}}{\overset{k_3}{\rightleftharpoons}} C^-$$

$$B^- + CH \underset{k_6}{\overset{k_5}{\rightleftharpoons}} BH + C^-.$$

TABLE 1 The rate of proton relaxation in various membranous systems

Object	Size	Reaction	Time of proton relaxation: At the surface	Time of proton relaxation: Between the surface and the bulk	Reference
BR membranes	1 μm	Proton release by BR (6°C)	500 μs	>3 ms	(Drachev et al., 1984)
BR membranes	1 μm	Proton release by BR	250 μs	~1 ms	(Heberle et al., 1994)
BR micelles	6 nm	Proton release by BR	20 μs	130 μs	(Scherrer et al., 1994)
BR membranes	1 μm	Proton release by BR	70 μs	850 μs	(Alexiev et al., 1995)
Isolated RCs from *Rb. sphaeroides*	4 nm	Proton uptake on the reduction of the primary quinone Q_A	n.d.	200 μs	(Maroti and Wraight, 1997)
Chromatophores of *Rb. sphaeroides*	50 nm	Proton uptake on the reduction of the secondary quinone Q_B (pH 6.2)	90 μs	500 μs	(Gopta et al., 1999)
Thylakoids	600 nm	Proton uptake on the reduction of Q_B in photosystem II	300 μs	3.3 ms	(Haumann and Junge, 1994b)
Spheroplasts of *Rb. sphaeroides*	2 μm	Proton release by the cytochrome-bc_1 complex	3 ms	70 ms	(Arata et al., 1987)
Cells of *Rb. capsulatus*	3 μm	Proton release by the cyochrome-bc_1 complex	3 ms	50 ms	(Jones and Jackson, 1989)
Spheroplasts of *Rb. sphaeroides*	2 μm	Proton release by the cytochrome-bc_1 complex	4 ms	30 ms	(Jones and Jackson, 1990)
Right-side-out vesicle of *Rb. Sphaeroides*	100 nm	Proton release by the cytochrome-bc_1 complex	4 ms	4 ms	(Jones and Jackson, 1990)

Because of the small buffer capacity of water, we did not consider the direct interaction of H^+ and OH^- ions in the presence of other buffers. The rate constants used for the reactions in the bulk phase are listed in Table 2 (the concentration of neutral water was included in the pseudo-first-order rate constants); other details are given in Appendix A.

The potential energy of a charged molecule at the membrane/water interface, $U(r)$, differs from its value in the bulk phase. Several factors can alter the potential energy near the interface: the electrostatic effect of surface charges, the decrease of the Born solvation energy near the membrane (image forces), the altered molecular structure of water at the surface, and the low dielectric permittivity of the interfacial water. Acting together, these effects lead to the appearance of a potential barrier in the water phase some 1 nm away from the surface (Cherepanov et al., 2003). As known from Kramers escape theory (Hänggi et al., 1990), the rate of diffusion through a potential barrier depends exponentially on the barrier height and is reciprocal to the curvature in the bottom of potential well and on the top of barrier. The anharmonic barrier corrections have only a minor effect on the escape rate (Talkner, 1995). As long as the exact form of the barrier was not known and its width might vary in the range of 2–5 nm, we approximated the potential energy for each chemical species i by a symmetric model function

$$U_i(r) = \begin{cases} 0.5U_i^{\max} \times [1 - \cos(\pi(r-R)/L)], & R \le r \le R + 2L \\ 0 & \text{otherwise} \end{cases}. \quad (7)$$

The function contains two adjustable parameters: the characteristic length of the interfacial region L (taken equal to 2 nm for all species) and the height of the barrier $U_i^{\max}$. Beyond a distance of $2L$ from the surface the potential was zero. The barrier height might depend on the electric charge, the size and geometrical form and on the chemical properties (like polarity and hydrogen bonding structure) of the mobile species. To reduce the number of fit parameters, we assumed the same height of the potential barrier both for the protonated and deprotonated form of a mobile buffer. Indeed, the total proton flux mediated by a mobile buffer includes two equal contributions: the protonated form of buffer moves in one direction and the deprotonated one moves in the opposite direction. Even if the protonated and deprotonated forms have different mobility at the interface, the total kinetic competence of the buffer in establishing proton equilibrium is determined by the slowest form. The patched distribution of positive and negative charges on the surface, which has been considered in our previous article (Cherepanov et al., 2003), was ignored for simplicity.

The evolution in time was described by the system of diffusion equations with the source terms responsible for the chemical interconversions of the species. For spherical membrane vesicles, the equations had the following form:

$$\frac{\partial c_i}{\partial t} = \frac{D_i}{r^2}\frac{\partial}{\partial r} r^2 \left(\frac{\partial c_i}{\partial r} + (k_B T)^{-1} \frac{\partial U_i}{\partial r} c_i \right) + \textit{Chemical Terms}.$$

Here the first term is the one-dimensional Smoluchowski equation in spherical coordinates, c_i is the concentration, D_i the diffusion coefficient, and $k_B T$ the thermal energy; the exact form of chemical terms was determined in accordance with the scheme of chemical interconversions (see Appendix A for details). The system of five partial differential equations was solved numerically by the algorithm described in Blom and Zegeling (1994). The size of the bulk phase was limited in such a way that the total amount of soluble buffer was at least 10-fold greater than the total amount of the fixed buffer on the membrane surface. The typical grid size was 20-fold greater than the radius of particles R, and the grid spacing was 20-fold smaller than the length of the interfacial region L; the boundaries were considered as impermeable for all kinds of particles.

The membrane sheets were approximated by flat horizontal cylinders. In cylindrical coordinates the respective diffusion equations had the form

$$\frac{\partial c_i}{\partial t} = \frac{D_i}{r}\frac{\partial}{\partial r} r \left(\frac{\partial c_i}{\partial r} + (k_B T)^{-1} \frac{\partial U_i}{\partial r} c_i \right) + D_i \left(\frac{\partial^2 c_i}{\partial z^2} + (k_B T)^{-1} \frac{\partial U_i}{\partial z} c_i \right) + \textit{Chemical Terms}.$$

The numeric solution was obtained by the adaptive grid solver for parabolic partial differential equations VLUGR2 (Blom et al., 1996) analogously to the solution in spherical coordinates.

The influence of membrane geometry on the proton relaxation dynamics

In the following sections, we analyzed experimental data on proton relaxation as obtained with membrane particles of different form: i), spherical membrane vesicles from phototrophic bacteria (chromatophores), and ii), bacteriorhodopsin containing flat membrane sheets (purple membranes). To check how the difference in membrane geometry affects the rate of proton relaxation, we calculated the latter for: i),

TABLE 2 Rate constants for the protolytic reactions in homogeneous aqueous solution

k_1* M^{-1} s^{-1}	k_{2B} s^{-1}	k_{2C} s^{-1}	k_3* $M^{-1}s^{-1}$	k_{4B} s^{-1}	k_{4C} s^{-1}	k_5 M^{-1} s^{-1}	k_6* M^{-1} s^{-1}
4×10^{10}	$4 \times 10^{10\text{-}pK_B}$	$4 \times 10^{10\text{-}pK_C}$	2×10^{10}	$2 \times 10^{pK_B\text{-}4}$	$2 \times 10^{pK_C\text{-}4}$	$10^{9+pK_B\text{-}pK_C}$	10^9

*The kinetic parameters k_1, k_3, and k_6 were taken from Chapter 7 of Bell (1973).

spherical vesicles of radius $R_{sph} = 354$ nm, and ii), flat cylindrical membrane sheets of radius $R_{cyl} = 500$ nm (typical for BR membranes). The full surface area of both types of particles (including both sides for unsealed membrane sheets) was identical and equal to 1.57×10^6 nm^2. In calculations we used, here quite arbitrary, the surface buffer capacity for BR membrane sheets of 7.4×10^{-8} mol m^{-2} estimated from the data of Grzesiek and Dencher (1986) as described below. We calculated the proton relaxation dynamics in the presence of 100 μM of a mobile pH buffer ($pK_C = 7.2$) with a diffusion coefficient $D_C = 2 \times 10^{-6}$ cm^2/s. The effect of interfacial potential barrier was not considered in these calculations.

The system was shifted out of the equilibrium by a fast and uniformly distributed ejection of protons on the membrane surface, after which the relaxation dynamics was calculated by numerical integration of the system of diffusion equations. The amount of protons transferred at a given time was calculated from the distribution of the protonated form of mobile buffer. The dynamics of surface/bulk equilibration for the cylindrical membrane sheet and for the spherical vesicle of the same area are shown in Fig. 1 by squares and circles, respectively. The rate of equilibration did not depend on the quantity of ejected protons. The dynamics of proton transfer in the flat sheet was somewhat faster during the first few microseconds after the ejection, but the general kinetic patterns became very similar already after 10 μs. The acceleration of proton transfer in the case of flat membrane sheet as compared to the spherical vesicle could be explained by a more dispersed volume distribution of fixed buffer in the former case. The calculated difference in the proton relaxation rate constant (by a factor of 1.5) was minor and of the same order as the scatter of data as measured by pH dyes (see, e.g., Heberle (1991)). Because of this reason, we used the spherical model throughout our further calculations as a more handy one.

For comparison, the dashed line in Fig. 1 shows the proton transfer dynamics calculated by the asymptotic Eq. 6. Apparently, the asymptotic solution overestimates the time of proton relaxation by a factor of 2 and predicts a twofold steeper time dependence than the exact numeric solution.

Dependence of the proton relaxation time on the vesicle size

Fig. 2 shows the dependence of the relaxation time on the concentration of mobile pH buffer as calculated for vesicles of various size (their radii are indicated at the plot; the diffusion coefficient of H_3O^+/OH^- ions and of the mobile buffer were assumed to be 10^{-4} cm^2 s^{-1} and 2×10^{-6} cm^2 s^{-1}, respectively; the potential barrier was assumed to be 60 meV both for H_3O^+/OH^- and for the mobile pH buffer). The plot in Fig. 2 shows that the proton relaxation time depends linearly on the radius of vesicles at concentrations of mobile buffer below 10^{-4} M, in agreement with the asymptotically derived Eq. 6. At high buffer concentrations ($>10^{-3}$ M) the relaxation time becomes independent of the radius because the depletion layer is then thinner than the radius of the vesicles.

The dependence of relaxation time on the geometrical size of membrane particles has been observed experimentally. An almost linear relationship has been reported for the proton release from the surface of *Rb. sphaeroides* membranes: in the suspension of whole spheroplasts with the diameter of ~ 2 μm the response of the externally added pH indicator cresol red occurred at 30 ms, whereas in the case of right-side-out vesicles with the diameter of ~ 100 nm, which were

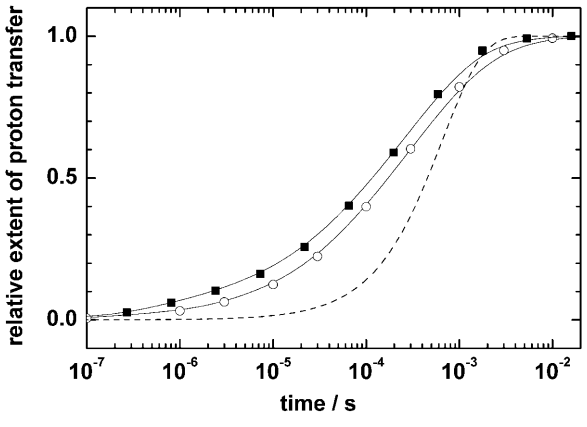

FIGURE 1 Calculated time course of surface/bulk proton equilibration in flat cylindrical membrane sheets (■) and spherical vesicles (○) of the same surface area. The radius of sheets and vesicles was 500 and 354 nm, respectively; the surface capacity of fixed buffer was 7.4×10^{-8} mol m^{-2}; the concentration of mobile buffer ($pK = 7.2$) was 100 μM; the diffusion coefficient of mobile buffer was 2×10^{-6} cm^2 s^{-1}, pH 7.2. The dashed line represents the monoexponential kinetics with the time constant calculated for the same parameters as Eq. 6.

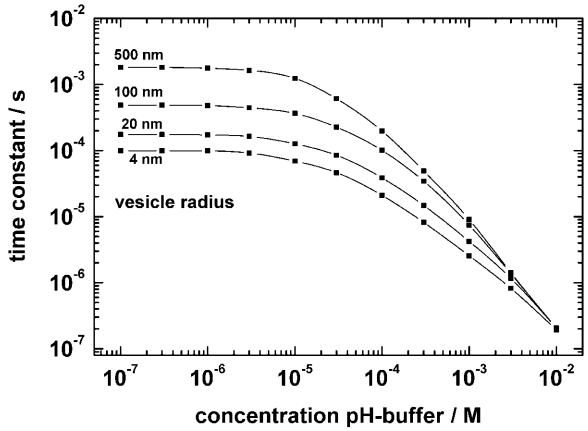

FIGURE 2 Dependence of proton relaxation time on the concentration of added mobile pH buffer as calculated for vesicles of various size. The radii in nm are indicated at the left of the curves; the diffusion coefficients of H^+/OH^- ions and of the mobile buffer were 10^{-4} cm^2 s^{-1} and 2×10^{-6} cm^2 s^{-1}, respectively; the potential barrier was 60 meV, both for the H^+/OH^- ions and for the mobile pH buffer.

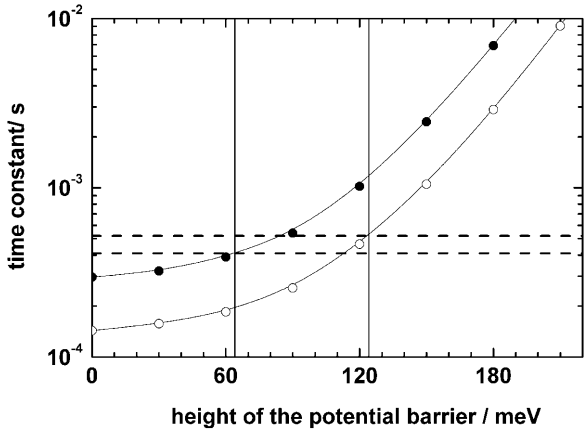

FIGURE 3 Estimation of the interfacial potential barrier for H^+/OH^- ions from the rate of BCP protonation in chromatophores of *Rb. sphaeroides*. The dependence of the proton relaxation time on the barrier height was calculated as described in the text using the surface buffer capacity of 1.2×10^{-7} mol m^{-2} (○) and 2.8×10^{-7} mol m^{-2} (●) and taking the thickness of the interfacial layer of 2 nm and the diffusion coefficient of H^+/OH^- ions of 10^{-4} cm^2s^{-1}. The chromatophore radius of 18 nm was assumed at calculations. The experimentally determined time constant of proton relaxation in chromatophores from *Rb. sphaeroides* (450 ± 50 μs) is shown by dashed horizontal lines. Vertical lines mark the interval for the estimated potential barrier of 65–125 meV consistent with the experimental data.

obtained by disruption of the spheroplasts, the same reaction proceeded at 4 ms (Jones and Jackson, 1990) (see Table 1). In the latter case, the proton release rate was apparently limited by the turnover of the cytochrome bc_1 complex, so that the genuine rate of protonic relaxation could be even faster.

A qualitatively similar behavior was observed also for the proton release by flat BR membranes and for the proton binding by photosynthetic reaction centers of *Rb. sphaeroides*. In both cases, the rate of proton relaxation was faster in preparations of the detergent-solubilized enzymes as compared with membrane preparations (see Table 1 for time constants and references). One has to take into account, however, that in these cases the transition to the detergent-solubilized preparation was likely to be coupled with the change in the surface buffering capacity, which can be hardly quantified.

Proton relaxation in chromatophores from purple bacteria

As shown in our previous work (Cherepanov et al., 2003), the height of the potential barrier in the interfacial layer with the low dielectric permittivity is determined largely by the electric charge and the effective radius of penetrating ions. The macroscopic approach is, however, rather imprecise in the treatment of molecular interactions at very short distances, so the effective radius of ions in the Born theory can significantly differ from the apparent geometrical radius calculated by the van der Waals volume of the molecule. Especially difficult is the case of H_3O^+ and OH^- ions because of strong hydrogen bonding in the first solvation layer of these species. Because of this uncertainty, we estimated the height of the potential barrier for H_3O^+ and OH^- ions by using our own experimental data on proton equilibration in preparations of chromatophore vesicles from *Rb. sphaeroides* and *Rb. capsulatus* (Gopta et al., 1999).

Chromatophores are sealed membrane vesicles of a radius of 15–30 nm. They are obtained from native invaginations of the plasma membrane after the disruption of bacterial cell. Excitation of chromatophores by a flash of light causes a charge separation in the photosynthetic reaction center followed by the reduction of the secondary quinone acceptor Q_B (see Okamura et al. (2000) for a review of the RC operation). The reduction of Q_B causes a proton transfer from the protein surface to the buried binding site at <100 μs. pH indicators in the bulk respond to this event only with delay; depending on the pH, the response time varied between ~450 μs and 1 ms at $6.2 < pH < 8.1$ in the presence of 300 mM KCl (see Gopta et al. (1999) for further details). At pH 6.2, the response time of the pH indicator bromocresol purple (BCP) was independent of its concentration up to 100 μM. The addition of the mobile pH buffer MES gradually diminished the extent of the BCP response. From the dependence of the extent of BCP response on the concentration of MES the buffer capacity of washed chromatophores at pH 6.2 could be estimated as 12 μM (Gopta et al., 1999), that corresponds to 100 buffer groups with pK 6.2 per one RC. This was an upper estimate for two reasons. First, ~10–20 μM of residual HEPES ($pK = 7.5$), which was used as pH buffer during the chromatophore preparation, was expected to remain even after a double washing of chromatophores in a buffer-free medium and to contribute, together with the fixed surface buffers, to the overall buffer capacity of the sample. Second, as long as the suspension medium was not degassed, a certain pH-buffering contribution from the dissolved carbon dioxide could be expected. Because the hydrolytic reaction of carbon dioxide is slow (the time constant is about ~0.3 s^{-1} (Drachev et al., 1984)), the latter contribution should be rather small on the timescale of pulsed measurements (1 ms).

The chromatophores from *Rb. sphaeroides* with mean radius of 18 nm were shown to carry 11 RC per vesicle, on average (with an error of ±30%); see Packham et al. (1978). Taking into account the uncertainties in the number of RC per vesicle and in the contribution from residual pH buffers, the surface buffer capacity of the external side of the membrane could be estimated to lie in the range between 1.2×10^{-7} mol m^{-2} and 2.8×10^{-7} mol m^{-2}. We calculated the time of proton equilibration for different potential barriers (varied in the range of 0–240 meV). The respective curves are plotted in Fig. 3. The open circles correspond to the lower estimate of the surface capacity (1.2×10^{-7} mol m^{-2}), and the solid circles correspond to the upper one (2.8×10^{-7} mol m^{-2}). The experimentally determined proton relaxation time

range of 450 ± 50 μs is shown by two dashed horizontal lines. The intersection of the theoretical and experimental curves gives an estimate for the potential barrier of 65–125 meV (shown by *vertical lines*).

Dependence of the proton relaxation time on the concentration of mobile buffer

Fig. 2 illustrates the expected dependence of the relaxation time on the concentration of mobile pH buffer in the presence of a 60-meV potential barrier. The accelerating effect of mobile buffer becomes pronounced only when their concentration exceeds a ''threshold'' value, here $\sim 10^{-5}$ M. As already noted, the inspection of published data, as obtained with different membrane preparations, showed that the ''threshold'' concentrations, at which pH buffers started to accelerate pH relaxation, varied in a rather wide range and correlated with the electrical charge of mobile species. For the singly charged *p*-nitrophenol and MES the threshold concentration was $\sim 10^{-5}$ M (Drachev et al., 1984; Porschke, 2002). Most of the tested pH buffers, e.g., the doubly charged phosphate, caused pronounced acceleration of proton relaxation only when added at $\geq 10^{-4}$ M (Drachev et al., 1984; Grzesiek and Dencher, 1986; Heberle, 1991; Haumann and Junge, 1994b; Maroti and Wraight, 1997; Gopta et al., 1999; Porschke, 2002). In the case of pyranine, with four negative charges in the deprotonated state, the threshold concentration was not reached in experiments because the high concentrations caused an impractically high absorption of the sample (Heberle, 1991; Porschke, 2002).

The ''threshold'' concentration depends on the ratio between the diffusional mobility of the buffer and the one of H^+/OH^- ions in the interfacial water layer. The mobility is determined in turn by the diffusion coefficient and the height of the potential barrier for the respective mobile species. Because the diffusion coefficients of mobile pH buffers/dyes in water vary in a rather narrow range being 10–50 times smaller than the diffusion coefficient of the proton (Baur and Wightman, 1991; Culbertson et al., 2002), the height of the potential barrier can be inferred from the threshold concentration. It is noteworthy that the ''threshold'' concentration is essentially independent of the surface buffer capacity and of the size of the vesicles. Moreover, it is even possible to compare data obtained at different experimental conditions after their normalization (i.e., multiplication of the rate by a constant factor).

The proton relaxation has been extensively studied with BR membrane sheets (reviewed by Heberle (2000)). The circles in Fig. 4, *A* and *B*, show the time of proton relaxation as measured at different concentrations of pH indicator pyranine, which was the only mobile proton carrier in the experimental system (the *solid circles* show the data of Porschke (2002) whereas the *open circles* the data of Heberle (1991)); the data sets were shifted along the *y*-axis to match the theoretical curves). The rate of proton relaxation was

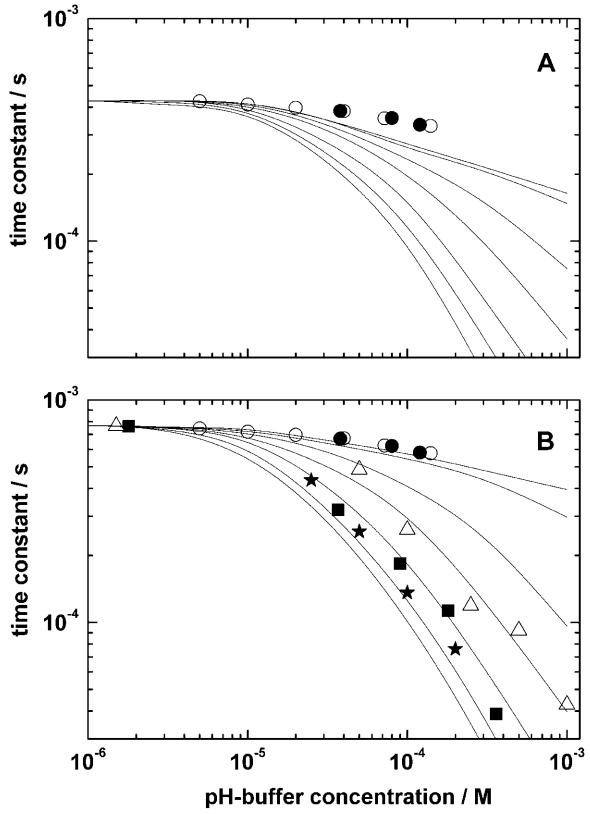

FIGURE 4 Dependence of proton relaxation time on the concentration of added mobile buffer. Each set of seven theoretical curves was calculated for various heights of potential barrier for mobile buffer, U_C^{max} (the values U_C^{max} = 0, 60, 120, 150, 180, 240, and 360 meV correspond to the curves plotted sequentially from the left to the right) at a given value of the potential barrier U_H^{max} for H^+ ions. All curves were calculated for vesicles of 100 nm radius and for the surface buffer capacity of 7.4×10^{-8} mol m^{-2}, pH 7.2. The time constants of experimentally measured pyranine protonation by the BR-ejected protons are shown by circles (*solid circles* represent the data from Porschke (2002) and *open circles* correspond to data from Heberle (1991)). (*A*) $U_H^{max} = U_{OH}^{max} = 0$; (*B*) $U_H^{max} = U_{OH}^{max} = 120$ meV. The response time of *p*-nitrophenol (Drachev et al., 1984) is shown by stars, the acceleration of proton relaxation (as measured by pyranine) by added MES (Porschke, 2002) and phosphate (Grzesiek and Dencher, 1986) is shown by squares and triangles, respectively. In the case of MES, the effective buffer capacity at the ambient pH of 7.45 was recalculated by using the buffer *pK* value of 6.2. The diffusion coefficient of H_3O^+/OH^- ions and of the mobile buffer were assumed to be 10^{-4} cm^2 s^{-1} and 2×10^{-6} cm^2 s^{-1}, respectively. The response time of indicators in the bulk was recalculated from the experimental kinetics by accounting for the time needed by BR to eject a proton under given experimental conditions.

almost independent of the concentration of pyranine, apparently because of poor ability of the highly charged pyranine anions (total charge −4) to penetrate the interfacial layer. Fig. 4 shows sets of theoretical curves, which were calculated for two different heights of the potential barrier for H^+ ions, U_H^{max}, and for different heights of the potential barrier for mobile buffer, U_C^{max}. Because the difference between proton relaxation dynamics as calculated for flat sheets and spherical vesicles was minor (see Fig. 1), and because the computation for the flat sheets was more

involved, especially in the presence of a potential barrier, the curves were calculated for spherical vesicles of 100 nm radius and a surface buffer capacity of 7.4×10^{-8} mol m^{-2} (pH 7.2). The value of the latter was estimated as follows: the total buffer capacity of the suspension of purple membranes, which contained 10 μM bacteriorhodopsin and 50 μM pyranine, can be estimated as 37 μM at pH 7 from data of Grzesiek and Dencher (1986). Subtracting the buffer capacity of pyranine at given pH (27 μM), we obtained a total surface buffer capacity for both sides of membrane of 1.0 mol/mol of BR. Taking the surface area of 11 nm^2 per monomer of BR (Essen et al., 1998) and assuming that both sides of membrane have similar capacity, we got the surface buffer capacity of 7.4×10^{-8} mol m^{-2}. This is the upper estimate because the membrane suspension might contain some residual extrinsic buffers besides pyranine (see above).

The steepest curve in Fig. 4 *A* was calculated in the absence of potential barriers for both H^+ and mobile buffer ($U_H^{max} = 0$ and $U_C^{max} = 0$). It gives the expected behavior for the commonly used model of a discontinuous ε at the membrane/water interface (see above). The slow rate of proton relaxation ($\sim$400 μs at low concentration of mobile buffers) comes in this case entirely from the damping effect of the fixed pH buffers at the membrane surface. As expected, the threshold concentration of mobile buffer is in this case $\sim 10^{-5}$ M.

The set of curves in Fig. 4 *A* demonstrates how the increasing potential barrier for mobile buffer slows down the proton equilibration (the values $U_C^{max} = 0, 60, 120, 150, 180, 240$, and 360 meV correspond to the curves plotted sequentially from the left to the right, respectively). Qualitatively, the higher is the potential barrier the weaker is the dependence on the buffer concentration. It is remarkable, however, that the impact of the barrier is relatively small and has a tendency to saturate: proton relaxation at $U_C^{max} = 240$ meV is almost as slow as at 360 meV. The underlying mechanism can be described as follows: the high potential barrier suppresses the direct interaction of the mobile buffer with the surface, so that the proton flux in the interfacial layer of $\sim$1 nm thickness is mediated mainly by the diffusion of H^+ ions proper. Therefore the further increase in the barrier height for buffer, starting from a certain value, has only a minor effect on the H^+ flux across the interfacial layer. Beyond the interfacial layer, however, the mobile buffer, the concentration of which greatly exceeds the concentration of H^+ ions, mediates the proton flux accounting for the residual weak dependence of proton relaxation rate on the concentration of the buffer. The experimental dependence for pyranine is shown in Fig. 4 *A* by circles. It is essentially flatter than the theoretical curve calculated with the maximal barrier $U_C^{max} = 360$ meV.

Apparently, the negligible dependence of proton relaxation on concentration of pyranine cannot be explained by the effect of potential barrier for pyranine alone and indicates the presence of a potential barrier for H^+/OH^- ions as well. In such case, the total proton flux would be limited by the H^+ diffusion through the interfacial layer and not by the diffusion in the bulk phase, where it can be accelerated by addition of pyranine. We calculated the analogous set of curves with the potential barrier $U_H^{max} = U_{OH}^{max} = 60$ meV (not documented). The barrier made the dependence on the concentration of mobile buffer less steep, but this was not sufficient to explain the negligible dependence on the concentration of pyranine. Only when the barrier for H^+/OH^- ions was increased up to 120 meV, the slowest theoretical curve calculated for the barrier with $U_C^{max} = 360$ meV became consistent with the experimental data (see Fig. 4 *B*). It is noteworthy that the calculated time of pyranine protonation of 800 μs in Fig. 4 *B* matches the experimentally measured one (700–1000 μs depending on conditions (Grzesiek and Dencher, 1986; Heberle, 1991; Porschke, 2002)). Thus, the quantitative consideration of proton relaxation in the preparations of BR membranes at different concentrations of pyranine provided the estimates of the barrier height for H^+/OH^- ions of $\geq$120 meV and for pyranine of $\geq$360 meV.

Several sets of experimental data for other pH buffers/mediators as obtained with the BR membranes are superimposed on the theoretical curves in Fig. 4 *B*. Because the experimental data were obtained at slightly varying conditions, each data set was shifted in the vertical direction to the position where its slope was equal to the slope of the respective theoretical curve. The stars represent the time of proton equilibration at different concentrations of pH indicator *p*-nitrophenol as measured by Drachev and coworkers (1984). Contrary to the pyranine case, the proton relaxation was accelerated already when the concentration of *p*-nitrophenol was increased from 25 μM to 50 μM. Two more data sets, which describe the acceleration of pyranine response in the bulk by added pH buffers, are plotted in Fig. 4 *B*: the triangles show the dependence of the pyranine response time on added phosphate (Grzesiek and Dencher, 1986) and the squares document the acceleration by added MES (Porschke, 2002). Because pyranine apparently could not get across the interfacial layer, these data allowed to estimate the height of the interfacial barrier for phosphate and MES, respectively. The height of the potential barrier was acquired from the shape of the curves in Fig. 4 *B* by assuming the same diffusion coefficient of 2×10^{-6} cm^2 s^{-1} for all mobile buffers. This procedure yielded the figure of $\sim$90 meV for *p*-nitrophenol and MES, $\sim$150 meV for phosphate, and $\geq$360 meV for pyranine, respectively.

We made analogous calculations for the acceleration of proton relaxation by mobile buffers in chromatophores from *Rb. sphaeroides* (shown in Fig. 5). The response times of BCP as function of its concentration (Gopta et al., 1999) are plotted in Fig. 5 by diamonds. One can see that at $<$100 μM the response of BCP was almost independent of its concentration. The response could be, however, accelerated by the addition of MES. Correspondingly, the open squares show

the dependence of the proton relaxation time on the concentration of MES as revealed from the kinetics of 20 μM BCP protonation (data from Gopta et al. (1999)). The comparison with the theoretical curves (the respective barrier heights in meV are indicated near the curves) yielded the potential barrier height of ~120 meV for MES and ~180 meV for BCP, respectively. The estimate for MES is in agreement with the estimate of 90 meV as obtained above for the BR membranes. The figure of 180 meV for BCP (the deprotonated form of which has the electric charge of −2) is consistent with the barrier of 150 meV as obtained above for the similarly charged phosphate.

Relationship between the height of potential barrier and the electric charge of penetrating ions

All pH buffers considered in Figs. 4 *B* and 5 were negatively charged in their deprotonated state: *p*-nitrophenol and MES had the total charge of −1, phosphate and BCP of −2, and pyranine of −4, respectively. In Fig. 6 we plotted the barrier height, as revealed here from the accelerating efficiency of mobile buffers, versus the charge of mobile species (the symbols in Fig. 6 correspond to the symbols in Figs. 4 *B* and 5). Despite some scattering, the dependence on the electric charge looked almost linear.

In the previous work (Cherepanov et al., 2003) we considered the interfacial water layer using: i), the empirical spatial dependence of dielectric permittivity as obtained by the atomic force microscopy at the mica surface (Teschke et al., 2001), and ii), the primitive electrolyte model, which neglects spatial correlations in the molecular structure of solvent (see e.g., Varela et al. (2003)) for a review of restrictions inherent to this kind of model). Applying the linear Poisson-Boltzmann equation with the varying dielectric permittivity, we calculated the potential energy profile for a singly charged spherical ion with radius of 0.25 nm. We found a potential barrier of 150–200 meV at 0.5–1 nm from the surface in the electrolyte solution (ionic strength of 0.1 M). Because the Born self-energy contribution is roughly proportional to the square of electric charge and to the inverse radius of penetrating ion, it was worthwhile to compare the estimates of potential barrier as obtained: a), from the analysis of the data on proton relaxation, with b), those calculated by the primitive model of electrolyte.

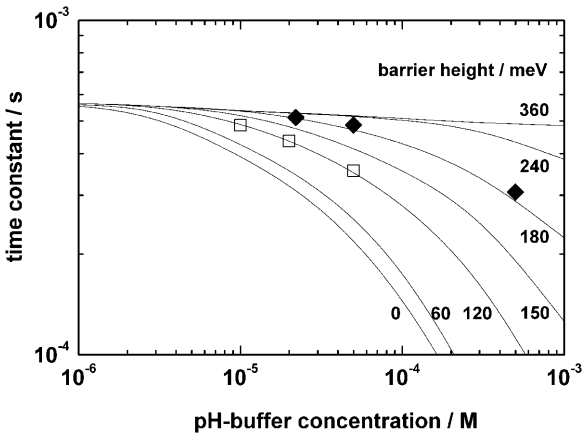

FIGURE 5 Acceleration of the proton relaxation in chromatophores from *Rb. sphaeroides* by mobile buffers. The response time of BCP is shown by circles and the acceleration of the 20-μM BCP response by MES is shown by squares (the experimental data were taken from Gopta et al. (1999) and corrected for the time of proton transfer from the surface to Q_B of 100 μs); the set of seven curves was calculated for the various heights of the potential barrier for mobile buffer (U_C^{max} = 0, 60, 120, 150, 180, 240, and 360 meV correspond to the *curves* plotted sequentially from the *left* to the *right*) using the potential barrier for H^+/OH^- ions $U_H^{max} = U_{OH}^{max} = 120$ meV.

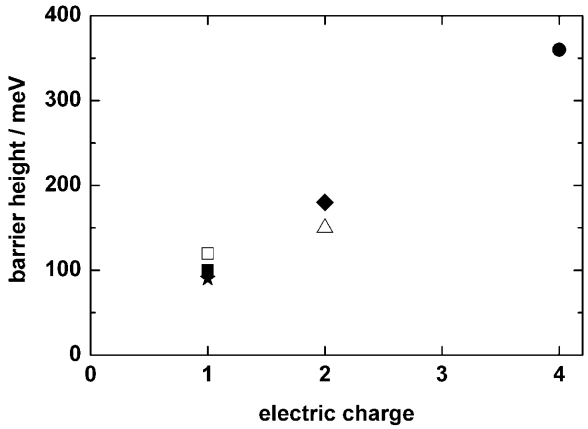

FIGURE 6 The height of interfacial barrier for five anionic pH buffers/indicators as function of their electric net charge in the deprotonated state. The barrier height was determined from the ability of buffers to accelerate proton equilibration at the membrane surface as described in the text. The symbols match those used in Figs. 4 *B* and 5.

The solvent accessible volume of *p*-nitrophenol (calculated by taking the van der Waals volume of molecule plus 0.14-nm-thick solvating shell) is 0.4 nm^3. Approximating the ellipsoidal molecule by a sphere of the same volume, one gets the effective radius of 0.46 nm. As long as the Born self-energy contribution to the potential barrier is expected to be proportional to the inverse radius of penetrating ions, the simple scaling of the barrier height calculated earlier for a sphere of 0.25 nm radius gives the estimate of 80–110 meV for the barrier height in the case of *p*-nitrophenol (method b), in agreement with the value of 90 meV as obtained by the data fit (method a). The solvent accessible volume of the sulfate group in MES, calculated in the same way, is 0.3 nm^3, so the barrier height as estimated by the primitive model comes in the range of 90–120 meV, again in agreement with the found value of 90–120 meV. It is noteworthy that a similar barrier height of ~120 meV was revealed here for the singly charged H^+/OH^- ions.

Coming to poly-charged species one had to take into account the actual shape of molecules, which can strongly deviate from the spherical form used in the previous calculations. It was especially important for the cases of

BCP and pyranine. Indeed, the molecule of BCP has a complicated shape where the negatively charged sulfate and hydroxy groups are separated by 0.8 nm from each other. The solvation energy of such distinct groups is roughly equal to the sum of two terms corresponding to the independent singly charged moieties. The respective estimate by the Born approach (method b) yielded the figure of 240–320 meV, somewhat exceeding the value of 180 meV as obtained from the concentration dependence (method a). Independent contributions are also expected for the case of pyranine anion carrying three sulfate and one hydroxy group. These charged groups are separated by 0.5–0.8 nm and can be considered as rather independent, so the height of potential barrier calculated by the Born theory is 360–480 meV, that is in agreement with the above estimate of ≥360 meV. Parted charges, however, cannot be invoked in the case of phosphate ion. It is a rather compact, almost spherical molecule having a solvent accessible volume of 0.28 nm^3. The Born approximation (method b) gave an estimate of 360–480 meV, exceeding more than twice the value of 150 meV, which was obtained by method a. The deviation might be due to several reasons. One possibility is that phosphate might adsorb at the membrane surface. Actually, some of the mobile buffers, as tested by Porschke (2002), showed an abnormally high ability to accelerate the proton equilibration between the BR surface and the bulk. Particularly, the data on boric acid and imidazole, when treated by the approach described above, could be described only under an assumption that their mobility in the interfacial water layer exceeded their mobility in bulk phase. Most likely these data indicate a nonspecific adsorption of these species in the interfacial layer. In the case of imidazole, its adsorption to thylakoid membranes and an unusually high ability to accelerate the proton relaxation has been amply documented (Junge et al., 1978; Hong and Junge, 1983; Polle and Junge, 1989; Haumann and Junge, 1994a). Correspondingly, the phosphate adsorption at the surface would decrease the height of an apparent potential barrier. Another reason for the discrepancy might be the higher mobility of small phosphate anions as compared to other pH buffers/dyes under consideration. Because the same diffusion coefficient of 2×10^{-6} cm^2 s^{-1} was taken for all mobile buffers on analyzing the data in Fig. 4 *B*, the barrier height for phosphate could be underestimated. One has also to take into account the general inaccuracy of the Poisson-Boltzmann approach when applied to inhomogeneous interfacial systems. For example, the activity coefficient of K^+ ions is 0.76 when calculated by the Debye-Hückel theory for a homogeneous solution with the ionic strength of 0.1 M. However, in the interfacial water layer with the dielectric constant of ~8, the activity coefficient of K^+ would be as small as 0.003. The low coefficient of activity is just another notion of the low affinity of interfacial water for ions (in terms of chemical potential). It is known that the primitive models work poorly in solutions with low coefficient of activity because of strong intermolecular correlations (Varela et al., 2003). Moreover, the free energy of a charge near the interface is not simply proportional to the electrostatic potential (as it is assumed in the primitive self-consistent Poisson-Boltzman and Debye-Hückel theories) but includes also other contributions, particularly the change of self-energy in the low-dielectric medium, and various non-electrostatic interactions (like hydrophobic and hydrogen bonding forces). It is noteworthy that the strong molecular organization of interfacial water has been established by direct measurements of forces between mica surfaces, which revealed up to 10 strong oscillations with a period of ~0.25 nm propagating up to 3 nm from the interface (Israelachvili and Pashley, 1983). Such oscillating forces cannot be described in the framework of the primitive solvent model and require a more sophisticated microscopic consideration. Unless an adequate description of interfacial phenomena is developed, it seems reasonable to consider the interfacial potential barrier not as a rigorously defined physical term but rather as a phenomenological parameter, the magnitude of which could be inferred from the analysis of experimental data.

Summarizing, we conclude that the apparent height of the potential barrier, which was estimated from the ability of mobile pH buffers to accelerate the proton equilibrium at the membrane/water interface, revealed an almost linear correlation with the maximal electric charge characterizing the buffer at a given pH. The observed dependence might be rationalized in terms of the Poisson-Boltzmann theory under the assumption of the low dielectric permittivity of interfacial water.

Relation to the pH-jump experiments

We showed above that a wealth of data on proton relaxation at the membrane/water interface (see review by Heberle (2000) and the above cited references) could be understood in terms of an energy barrier arising in the surface water layer with altered dielectric properties. Despite numerous evidence indicating the presence of such a barrier (see citations above), the concept of anisotropic proton relaxation at the membrane surface has remained controversial, mainly because of the counter-argumentation based on pH-jump experiments (reviewed by Gutman and Nachliel (1995) and Brandsburg-Zabary et al. (2000)). These authors used short laser pulses to trigger photo-deprotonation of pyranine in the absence and in the presence of membrane preparations. In pure water, the photo-deprotonation of pyranine (at $\tau < 1$ ns) was followed by its reprotonation at few μs. In the presence of submitochondrial particles, however, the reprotonation became essentially biphasic: besides the major fast component, a new slower component with τ of ~30 μs appeared (Gutman et al., 1993). The authors explained the retardation of pyranine reprotonation by the transient interaction of the

photo-ejected protons with the membrane surface. Based on these and similar observations it has been concluded that the diffusion of protons between the membrane surface and the bulk occurs at tens of microseconds and that such a fast proton transfer excludes functionally relevant kinetic barriers at the interface (Gutman et al., 1993; Kotlyar et al., 1994; Gutman and Nachliel, 1995).

Analogous results as obtained with BR membranes were rationalized in a similar way (Nachliel et al., 1996; Checover et al., 1997). In the latter case, however, it has remained unexplained how it could happen that the protons, ejected by pyranine in the bulk phase, could reach the BR membrane and return back to the bulk phase at ~20–30 μs (making a full roundtrip), whereas the protons, which were ejected to the membrane surface by BR proper, needed as long as 1 ms for their one way trip to pyranine in the bulk (this behavior has been reported by several research groups (Heberle and Dencher, 1992; Drachev et al., 1992; Heberle et al., 1994; Alexiev et al., 1995; Dioumaev et al., 1998; Porschke, 2002)). Further on, the collision of protons ejected by pyranine in the bulk phase with the surface of membrane particle could occur only if pyranine resides in the surrounding water layer not farther than ~20 nm from the surface (the average distance between pyranine molecules in solution). One can easily calculate, taking the actual size of membrane particles and their usual concentration of a few nanomoles, that the probability of such reaction is $<2 \times 10^{-3}$. Correspondingly, the extent of the slow kinetic component of pyranine reprotonation is expected to be smaller than the extent of the fast component by three orders of magnitude, and not by a factor of 10, as it has been reported.

Fernandez and Politi (1997) asked whether the pyranine molecules, the reprotonation of which proceeded at 10–30 μs in such pH-jump experiments, were indeed dissolved in the bulk and not adsorbed at the membrane surface. They noted that if the negatively charged pyranine binds both to liposomes, even the negatively charged ones (Kano and Fendler, 1978; Clement and Gould, 1981), and to proteins (Sedgwick and Bragg, 1990; Gutman, 1986; Yam et al., 1991; Gutman et al., 1992), it might bind to the protein-containing membranes as well. And indeed, Ziegler and Penefsky (1993) have convincingly demonstrated that submitochondrial particles, similar to those used by Gutman and co-workers, retained significant amounts of pyranine at their outer surface even after they were passed through a Sephadex column. The presence of a membrane-absorbed/bound fraction of pyranine would affect the kinetics of its protolytic reactions in a quite predictable way. The pyranine in the water phase would be reprotonated at a few μs. The protons released by the fraction of pyranine adsorbed at the membrane surface would be transiently retained by surface buffers. In this fraction the reprotonation of pyranine would proceed in tens of microseconds. The kinetic trace of pyranine reprotonation would contain thereby two components with the characteristic time of few microseconds (in the bulk) and tens of microseconds (at the surface), as it was actually observed (Gutman et al., 1993; Kotlyar et al., 1994; Gutman and Nachliel, 1995; Nachliel et al., 1996; Checover et al., 1997). The relative extent of the slower component is expected to be roughly proportional to the relative amount of pyranine adsorbed at the membrane surface. Because the relaxation in both fractions completes at tens of microseconds, the proton transfer between the surface and the bulk, which has a characteristic time of 1 ms (Heberle et al., 1994, 2000), could not be revealed from the kinetics of pyranine reprotonation.

If some pyranine could adsorb at the BR surface, it was expected to be protonated by the BR-ejected protons faster than the major fraction in the bulk. In Appendix B we demonstrate that the published kinetic traces of pyranine protonation by the BR-ejected protons indeed contain a minor fast component with a rise time of ~300 μs matching the response time of fluorescein, which was covalently bound to BR. (One has to keep in mind that the proton ejection by BR proper takes $\geq$100 μs as compared to the proton ejection by photoexcited pyranine, which proceeds at $<$1 ns). The relative extent of the fast component is 10–20%, in good correspondence with the relative amplitude of the slower component in the pH-jump experiments.

Thus, the striking controversy between the time constants of pyranine protonation by the BR-ejected protons (1 ms) and of its reprotonation in the pH-jump experiments (tens of microseconds for the slower component) could be resolved by attributing the latter reaction to the surface adsorbed fraction of pyranine. Based on this consideration, we suggest that the data obtained in the pH-jump experiments do not contain information about proton exchange between the membrane surface and the bulk water phase and therefore cannot be considered as evidence against the slow rate of the proton equilibration between the membrane surface and the bulk water phase.

OUTLOOK AND CONCLUSIONS

The analysis presented in this work complements two previous reports. In the first one we have studied the repletion from the bulk of proton vacancies (holes) formed at the surface of chromatophore vesicles of *Rb. sphaeroides* and *Rb. capsulatus* in response to a light flash. We found that proton donation by bimolecular collision with soluble pH buffers was impeded at their concentration below 100 μM. The high activation energy of the proton relaxation (30–50 kJ at neutral pH) provided evidence for proton donation by neutral water (Gopta et al., 1999).

The possible nature of the potential barrier, which impeded the interaction of mobile pH buffers with the surface, was elucidated in the next article (Cherepanov et al., 2003), where we have shown that potential barrier could

result from the low dielectric permittivity of surface water, a phenomenon well known in electrochemistry (Bockris and Reddy, 1977) and recently corroborated by atomic force microscopy at the mica surface (Teschke et al., 2001).

It has remained an open question whether the properties of water at the mica surface apply to biological membranes. Elucidation of this question was the main goal of the present work. We attempted to ''extract'' the properties of the interfacial barrier by a comparative analysis of data obtained with various biological membranes and various pH buffers/indicators. We obtained a consistent picture where the ability of various mobile buffers to accelerate the proton equilibration between the surface and the bulk phase was correlated with their electric charge, which determined the height of the interfacial energy barrier as felt by these buffers.

Modeling showed that the rate of proton exchange between the surface of a membrane particle and the bulk is determined by the pH-buffering capacity of the surface, the size of the particle, and the height of the potential barrier. The importance of the surface buffering capacity for explaining the proton relaxation dynamics is well recognized (Junge and Polle, 1986; Junge and McLaughlin, 1987; Jones and Jackson, 1989). The dependence on the geometrical size of membrane particles and on the height of the interfacial potential barrier was revealed for the first time. It is noteworthy that the surface buffering capacity does not matter at steady state (Junge and Polle, 1986), so that only the height of the potential barrier and the size of membrane particles determine the surface proton activity. Because the potential barrier for proton proper is only on the order of 120 meV, the dependence on the size is especially relevant for understanding bioenergetics of bacteria, particularly of the alkaliphilic ones. The steric effects are expected to be minimal for the spherical particles, which we have considered on modeling; for membraneous structures with negative curvature (e.g., invaginations of the inner cellular membrane that are typical, e.g., for phototropic prokaryots) the contribution of steric factors to the retardation of proton transfer could be even larger.

The results presented in this work and in two preceding articles provide a rationale to solve the long lasting controversy between concepts of the localized and the fully delocalized proton coupling in biological energy transduction (see Williams (1978, 2001), Cramer and Knaff (1991), and Ferguson (1995, 2000) for comprehensive coverage of this controversy). It is possible to conclude that the relatively large size of bacterial cells and the presence of negatively charged groups at the bacterial surface act synergetically in keeping the proton concentration in the thin water layer around the cell higher than in the surrounding medium. Further biologically relevant implications, which follow from the apparent presence of the interfacial potential barrier for ions, are considered in detail in our previous article (Cherepanov et al., 2003).

The provided theoretical framework would hopefully facilitate experimental studies of interfacial phenomena. The membrane-adjoining water layer with thickness of ≤ 1 nm serves apparently as a cellular subcompartment, which is particularly important for energy coupling in bacteria because proton activity in this space can be independent of pH in the bulk water phase under steady turnover of proton pumps (Cherepanov et al., 2003). Hence, it seems worthwhile to tackle the properties of this surface water layer. It could be done by further varying the nature of penetrating ions, ionic strength, etc. Flash-triggered biological systems allow direct tracing of the partial steps of interfacial charge transfer by combining various techniques (see Drachev et al. (1984), Junge (1987), Heberle et al. (1994), Alexiev et al. (1995), and Gopta et al. (1999)). It is noteworthy, that such pulse measurements of charge transfer across the interface are hardly possible in chemical systems, so that biological membranes might serve as useful models in experimental studies of charge transfer across the interface.

After the manuscript was accepted for publication, we came across the recent article by Cheng and co-workers (2003) who have shown, by using coherent anti-Stokes Raman scattering microscopy, that at room temperature the majority of water molecules trapped between phospholipid bilayers in multilamellar onions was ordered. This finding corroborates our conclusion on the presence of a potential barrier at the surface of biological membranes due to the ordering of water molecules in the surface water layer.

APPENDIX A

We consider protolytic interaction and diffusion of four chemical species: 1), a fixed pH buffer B at the membrane surface; 2), a soluble pH buffer C in the bulk phase; 3), the hydrated proton H^+; and 4), the hydroxyl anion OH^-. The protolytic interactions in the system were represented by the scheme of five chemical reactions described in the main text. The fixed buffer B was assumed to be distributed in the surface layer of thickness L, its total concentration $P_{B0}(r)$ was approximated by the formula

$$P_{B0}(r) = \begin{cases} 0.5 \times P_{B0}^{max} \times [1 + \cos(\pi(r + L - R)/L)], \\ \qquad\qquad R - L \leq r < R \\ 0 \qquad\qquad r \geq R, \end{cases}$$

and did not change in time. The concentrations of protonated, $P_{BH}(r)$, and deprotonated, $P_B(r)$, forms of the surface buffer changed in time but their sum remained equal to $P_{B0}(r)$. By similar way $P_{CH}(r)$ and $P_C(r)$ denote the concentrations of the protonated and deprotonated forms of the mobile buffer (their sum $P_{C0}(r)$ may, however, change in time). In the modeling we considered also the hydrated proton H^+ and the hydroxyl anion OH^-; their concentrations were denoted by $P_H(r)$ and $P_{OH}(r)$, respectively.

The kinetic model included the system of five partial differential equations

$$\frac{\partial P_H}{\partial t} = \frac{D_H}{r^2}\frac{\partial}{\partial r} r^2 \left(\frac{\partial P_H}{\partial r} + (k_B T)^{-1} \frac{\partial U_H(r)}{\partial r} P_H \right) + Q_1$$

$$\frac{\partial P_{OH}}{\partial t} = \frac{D_{OH}}{r^2}\frac{\partial}{\partial r} r^2 \left(\frac{\partial P_{OH}}{\partial r} + (k_B T)^{-1} \frac{\partial U_{OH}(r)}{\partial r} P_{OH} \right) + Q_2$$

$$\frac{\partial P_{BH}}{\partial t}=\frac{D_{BH}}{r^2}\frac{\partial}{\partial r}r^2\left(2\frac{\partial P_{BH}}{\partial r}+(k_BT)^{-1}\frac{\partial U_{BH}(r)}{\partial r}P_{BH}\right)+Q_3$$

$$\frac{\partial P_{CH}}{\partial t}=\frac{D_{CH}}{r^2}\frac{\partial}{\partial r}r^2\left(2\frac{\partial P_{CH}}{\partial r}+(k_BT)^{-1}\frac{\partial U_{CH}(r)}{\partial r}P_{CH}\right)+Q_4$$

$$\frac{\partial P_{C}}{\partial t}=\frac{D_{C}}{r^2}\frac{\partial}{\partial r}r^2\left(\frac{\partial P_{C}}{\partial r}+(k_BT)^{-1}\frac{\partial U_{C}(r)}{\partial r}P_{C}\right)+Q_5.$$

The diffusion coefficient of the surface buffer D_{BH} was zero, and the concentration of its deprotonated form was calculated by the equation $P_B = P_{B0} - P_{BH}$. The potential energy of the protonated form of the mobile buffer was assumed equal to the energy of the deprotonated form ($U_{CH} = U_C$), similarly the potential energy of H^+ matched the energy of OH^- ($U_H = U_{OH}$). The chemical interactions between species were treated in accordance with the usual rules of chemical kinetics:

$$Q_1 = -k_1\times P_B\times P_H + k_{2B}\times P_{BH} - k_1\times P_C\times P_H + k_{2C}\times P_{CH}$$

$$Q_2 = -k_3\times P_{BH}\times P_{OH} + k_{4B}\times P_B - k_3\times P_{CH}\times P_{OH} + k_{4C}\times P_C$$

$$Q_3 = k_1\times P_B\times P_H - k_{2B}\times P_{BH} - k_3\times P_{BH}\times P_{OH} + k_{4B}\times P_B + k_5\times P_B\times P_{CH} - k_6\times P_{BH}\times P_C$$

$$Q_4 = k_1\times P_C\times P_H - k_{2C}\times P_{CH} - k_3\times P_{CH}\times P_{OH} + k_{4C}\times P_C - k_5\times P_B\times P_{CH} + k_6\times P_{BH}\times P_C$$

$$Q_5 = -k_1\times P_C\times P_H + k_{2C}\times P_{CH} + k_3\times P_{CH}\times P_{OH} - k_{4C}\times P_C + k_5\times P_B\times P_{CH} - k_6\times P_{BH}\times P_C.$$

APPENDIX B

Here we provide a quantitative analysis of two types of proton pulse experiments with BR membrane sheets. In one set of experiments, reproduced by several groups, protons were ejected by BR proper. The surface-bound pH indicator fluorescein reported the appearance of these protons at 100–300 μs (depending on the position to which it was bound). Another pH indicator, pyranine, when added to BR sheets, responded slower, at 700–1000 μs, depending on conditions (see Heberle (2000) for a review). In another set of experiments, protons were ejected by pyranine in response to a laser flash. Whereas in pure water pyranine was reprotonated at few microseconds, the presence of BR sheets led to the appearance of a minor component of pyranine reprotonation with characteristic time of 20–30 μs (Nachliel et al., 1996; Checover et al., 1997). This retardation has been explained by a transient ''trapping'' of protons, which were released by pyranine in the bulk, by the buffer groups at the surface of BR sheets. In the framework of this explanation, the *pK* of groups involved was calculated to be ~4.0–5.0 as long as the rate of proton release into water depends on *pK* of proton releasing group as $\sim 10^{11\text{-pK}}\ s^{-1}$.

As discussed in the main text, two sets of experiments stay in contradiction to each other. To our best knowledge no attempts to consider these two data sets simultaneously were conducted. The attempt of Nachliel and Gutman (1996) to explain the retarded interaction of the BR-ejected protons with pyranine (Heberle et al., 1994) by their retention at the surface by carboxyls with effective *pK* of ~5.0 raises several questions. First, the two-dimensional diffusion of protons along the surface of BR membranes and the proton equilibration between the surface and the bulk solution were treated in the framework of homogeneous chemical kinetics. Second, the data of Heberle and co-workers (1994) were fitted by a parameter set, which described a particular situation, where the interaction of pyranine with the cytoplasmic membrane side was postulated to be by three orders of magnitudes slower than with the extracellular surface, with rate constant of 10^7 and $5\times10^9\ M^{-1}s^{-1}$, respectively. No explanation for the three orders of magnitude difference in the diffusion-controlled interaction of pyranine with two surfaces of the unsealed BR membranes has been offered. Thereby the other fit parameters were chosen in such a way that they favored the prompt relocation of the ejected protons from the extracellular surface of BR to the cytoplasmic one and their dwelling at the latter. In our view, the parameter set, which allowed to fit the data of Heberle and co-workers (1994) implied, although indirectly, a diffusion barrier for pyranine at one of the membrane surfaces.

An alternative explanation follows from the suggestion of Fernandez and Politi (1997) that the pyranine molecules, the reprotonation of which proceeded at 10–30 μs in the case of pH-jump experiments were present not in the bulk water phase but at the membrane surface. Pyranine molecules, seemingly, have a high affinity to positively charged patches on the protein surface with a mixed hydrophobic/hydrophilic microenvironment (see references in the main text). As long as BR membranes contain >90% of protein, one can expect pyranine binding/adsorption in the case of these preparations as well. The presence of a membrane adsorbed pyranine fraction directly reveals itself as a minor, faster component in the kinetics of pyranine protonation by the BR-ejected protons, as documented in Fig. 7, where the kinetic traces of proton binding to the surface-attached fluorescein (bound to the residue 36 of BR) and of pyranine protonation in the same probe are replotted from the work of Heberle and co-workers (1994). The kinetic analysis revealed that the trace of pyranine protonation actually contained a fast component with a relative extent of ~20% and a rise time of 360 μs. The latter value matched the time constant of proton binding to fluorescein covalently attached to the BR surface in the same experimental setup (~330 μs). Two bottom plots in Fig. 7 show the residuals of one- and two-exponential fits of the pyranine protonation.

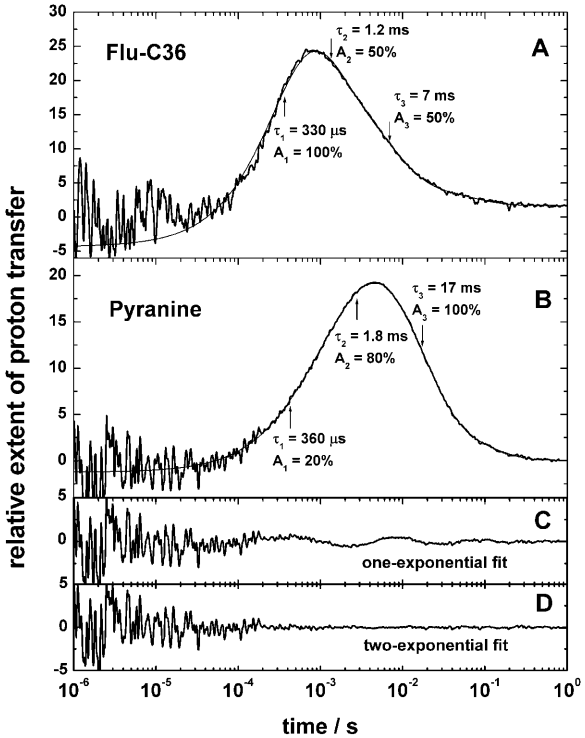

FIGURE 7 The multiexponential deconvolution of the proton relaxation kinetics at BR membranes (the kinetic traces were taken from Heberle et al. (1994)). (*A*) Proton binding to fluorescein covalently attached to the residue 36 in BR, replotted from Fig. 2 *b* in Heberle et al. (1994). (*B*) Proton binding to pyranine in solution (the same sample as in Fig. 7 *A*, replotted from Fig. 2 *d* in Heberle et al. (1994)). (*C*) Residual of the one-exponential fit of the proton binding to pyranine in Fig. 7 *B*. (*D*) Residual of the two-exponential fit of the proton binding to pyranine in Fig. 7 *B*.

Similar fast component with a relative extent of ~15% and a time constant of ~250 μs (not documented) was found in the kinetics of pyranine response published by Alexiev and co-workers (1995). Noteworthy, the extent of the relative extent of the fast pyranine protonation by BR in cited works (10–20%, depending on the fitting routine) correlates with the relative extent of the slow pyranine reprotonation in the pH-jump experiments with BR membranes (~10%; see Nachliel et al. (1996) and Checover et al. (1997)). The extent of the faster component of pyranine protonation seems to depend on experimental conditions: in the most recent article on pH-jump experiments with BR membranes the fast component of pyranine protonation was apparently present when the measurements were conducted in 150 mM KCl but absent when they were done in water (Schatzler et al., 2003). One can suggest that in the case of BR the interaction of pyranine with the membrane can be putatively described as a nonspecific adsorption and not as a relatively tight binding as in the case of submitochondrial particles (Ziegler and Penefsky, 1993) (see also the main text).

We are thankful to L. Drachev, M. Gutman, J. Hebele, L. Krishtalik, E. Nachliel, D. Oesterhelt, V. Skulachev, and M. Verkhovsky for useful discussions. This work is a direct outgrowth of our numerous discussions with the late Andrey Kaulen. Andrey was the first, together with Lel' Drachev and Vladimir Skulachev, who revealed the delay in proton transfer from the surface of biological membrane into the surrounding solution by following both the flash-induced proton displacement across the BR membranes and the absorption changes of a pH indicator in the bulk water phase.

This work was supported by the Alexander von Humboldt Foundation, the Volkswagen Foundation, the International Association for the Promotion of Cooperation with Scientists from the New Independent States of the former Soviet Union (INTAS) (2001-736), and by grants from the Deutsche Forschungsgemeinschaft (Mu-1285/1, Ju-97/13, SFB 431-P15, 436-RUS-113/210).

REFERENCES

Alexiev, U., R. Mollaaghababa, P. Scherrer, H. G. Khorana, and M. P. Heyn. 1995. Rapid long-range proton diffusion along the surface of the purple membrane and delayed proton transfer into the bulk. *Proc. Natl. Acad. Sci. USA.* 92:372–376.

Arata, H., I. Takenaka, and M. Nishimura. 1987. Flash-induced proton release in *Rhodopseudomonas sphaeroides* spaeroplasts. *J. Biochem.* 101:261–265.

Baur, J. E., and R. M. Wightman. 1991. Diffusion-coefficients determined with microelectrodes. *J. Electroanal. Chem.* 305:73–81.

Bell, R. P. 1973. The Proton in Chemistry. Chapman & Hall, London, UK.

Berry, R. S., S. A. Rice, and J. Ross. 1980. Physical Chemistry. Wiley, New York.

Blom, J. G., R. A. Trompert, and J. G. Verwer. 1996. Algorithm 758: VLUGR2: a vectorizable adaptive-grid solver for PDEs in 2D. *Acm Transactions on Mathematical Software.* 22:302–328.

Blom, J. G., and P. A. Zegeling. 1994. A moving-grid interface for systems of one-dimensional time-dependent partial differential equations. *ACM Trans. Math. Soft.* 20:194–214.

Bockris, J. O., and A. K. N. Reddy. 1977. Modern Electrochemistry. Plenum Press, New York.

Brandsburg-Zabary, S., O. Fried, Y. Marantz, E. Nachliel, and M. Gutman. 2000. Biophysical aspects of intra-protein proton transfer. *Biochim. Biophys. Acta.* 1458:120–134.

Checover, S., E. Nachliel, N. A. Dencher, and M. Gutman. 1997. Mechanism of proton entry into the cytoplasmic section of the proton-conducting channel of bacteriorhodopsin. *Biochemistry.* 36:13919–13928.

Cheng, J.-X., S. Pautot, D. A. Weitz, and S. Xie. 2003. Ordering of water molecules between phospholipid bilayers visualized by coherent anti-Stokes Raman scattering microscopy. *Proc. Natl. Acad. Sci. USA.* 100: 9826–9830.

Cherepanov, D. A., B. A. Feniouk, W. Junge, and A. Y. Mulkidjanian. 2003. Low dielectric permittivity of water at the membrane interface: effect on the energy coupling mechanism in biological membranes. *Biophys. J.* 2:1307–1316.

Clement, N. R., and J. M. Gould. 1981. Pyranine (8-hydroxy-1,3, 6-pyrenetrisulfonate) as a probe of internal aqueous hydrogen ion concentration in phospholipid vesicles. *Biochemistry.* 20:1534–1538.

Cramer, W. A., and D. B. Knaff. 1991. Energy Transduction in Biological Membranes: A Textbook of Bioenergetics. Springer, New York.

Culbertson, C. T., S. C. Jacobson, and J. M. Ramsey. 2002. Diffusion coefficient measurements in microfluidic devices. *Talanta.* 56:365–373.

Dioumaev, A. K., H. T. Richter, L. S. Brown, M. Tanio, S. Tuzi, H. Saito, Y. Kimura, R. Needleman, and J. K. Lanyi. 1998. Existence of a proton transfer chain in bacteriorhodopsin: participation of Glu-194 in the release of protons to the extracellular surface. *Biochemistry.* 37:2496–2506.

Drachev, A. L., A. D. Kaulen, and V. I. Skulachev. 1984. Correlation of photochemical cycle, H^+ release and uptake, and electric events in bacteriorhodopsin. *FEBS Lett.* 178:331–336.

Drachev, L. A., A. D. Kaulen, and A. Y. Komrakov. 1992. Interrelations of M-intermediates in bacteriorhodopsin photocycle. *FEBS Lett.* 313:248–250.

Elferink, M. G., I. Friedberg, K. J. Hellingwerf, and W. N. Konings. 1983. The role of the proton-motive force and electron flow in light-driven solute transport in *Rhodopseudomonas sphaeroides*. *Eur. J. Biochem.* 129:583–587.

Essen, L., R. Siegert, W. D. Lehmann, and D. Oesterhelt. 1998. Lipid patches in membrane protein oligomers: crystal structure of the bacteriorhodopsin-lipid complex. *Proc. Natl. Acad. Sci. USA.* 95: 11673–11678.

Ferguson, S. J. 1985. Fully delocalised chemiosmotic or localised proton flow pathways in energy coupling? A scrutiny of experimental evidence. *Biochim. Biophys. Acta.* 811:47–95.

Ferguson, S. J. 1995. Chemiosmotic coupling. Protons fast and slow. *Curr. Biol.* 5:25–27.

Ferguson, S. J. 2000. Proton transfer: it's a stringent process. *Curr. Biol.* 10:R627–R630.

Fernandez, C., and M. J. Politi. 1997. Effects of probe-amphiphile interaction on pyranine proton transfer reactions in lecithin vesicles. *Journal of Photochemistry and Photobiology A-Chemistry.* 104:165–172.

Georgievskii, Y., E. S. Medvedev, and A. A. Stuchebrukhov. 2002. Proton transport via the membrane surface. *Biophys. J.* 82:2833–2846.

Gopta, O. A., D. A. Cherepanov, W. Junge, and A. Y. Mulkidjanian. 1999. Proton transfer from the bulk to the bound ubiquinone Q_B of the reaction center in chromatophores of *Rhodobacter sphaeroides*: retarded conveyance by neutral water. *Proc. Natl. Acad. Sci. USA.* 96:13159–13164.

Grzesiek, S., and N. A. Dencher. 1986. Time-course and stoichiometry of light-induced proton release and uptake during the photocycle of bacteriorhodopsin. *FEBS Lett.* 208:337–342.

Guffanti, A. A., and T. A. Krulwich. 1984. Bioenergetic problems of alkalophilic bacteria. *Biochem. Soc. Trans.* 12:411–412.

Guffanti, A. A., M. Mann, T. L. Sherman, and T. A. Krulwich. 1984. Patterns of electrochemical proton gradient formation by membrane vesicles from an obligately acidophilic bacterium. *J. Bacteriol.* 159:448–452.

Gutman, M. 1986. Application of the laser-induced proton pulse for measuring the protonation rate constants of specific sites on proteins and membranes. *Methods Enzymol.* 127:522–38.

Gutman, M., A. B. Kotlyar, N. Borovok, and E. Nachliel. 1993. Reaction of bulk protons with a mitochondrial inner membrane preparation: time-resolved measurements and their analysis. *Biochemistry.* 32:2942–2946.

Gutman, M., and E. Nachliel. 1995. The dynamics of proton exchange between bulk and surface groups. *Biochim. Biophys. Acta.* 1231:123–138.

Gutman, M., Y. Tsfadia, A. Masad, and E. Nachliel. 1992. Quantitation of physical-chemical properties of the aqueous phase inside the phoE ionic channel. *Biochim. Biophys. Acta.* 1109:141–148.

Haumann, M., and W. Junge. 1994a. Extent and rate of proton release by photosynthetic water oxidation in thylakoids: electrostatic relaxation versus chemical production. *Biochemistry.* 33:864–872.

Haumann, M., and W. Junge. 1994b. The rates of proton uptake and electron transfer at the reducing side of photosystem II in thylakoids. *FEBS Lett.* 347:45–50.

Hänggi, P., P. Talkner, and M. Borkovec. 1990. Reaction-rate theory: fifty years after Kramers. *Rev. Mod. Phys.* 62:251–341.

Heberle, J. 1991. Zeitauflösende Untersuchung der Protonentranslokationsschritte von Bakteriorhodopsin mittels chemisch-gekoppelter pH-Indikatoren. Freien Universität, Berlin.

Heberle, J. 2000. Proton transfer reactions across bacteriorhodopsin and along the membrane. *Biochim. Biophys. Acta.* 1458:135–147.

Heberle, J., and N. A. Dencher. 1992. Surface-bound optical probes monitor protein translocation and surface potential changes during the bacteriorhodopsin photocycle. *Proc. Natl. Acad. Sci. USA.* 89:5996–6000.

Heberle, J., J. Riesle, G. Thiedemann, D. Oesterhelt, and N. A. Dencher. 1994. Proton migration along the membrane surface and retarded surface to bulk transfer. *Nature.* 370:379–382.

Hong, Y. Q., and W. Junge. 1983. Localized or delocalized protons in photophosphorylation? On the accessibility of the thylakoid lumen for ions and buffers. *Biochim. Biophys. Acta.* 722:197–208.

Israelachvili, J. N. 1992. Intermolecular and Surface Forces. Academic Press, London, UK.

Israelachvili, J. N., and R. M. Pashley. 1983. Molecular layering of water at surfaces and origin of repulsive hydration forces. *Nature.* 306:249–250.

Jones, M. R., and J. B. Jackson. 1989. Proton release by the quinol oxidase site of the cytochrome b/c_1 complex following single turnover flash exitation of intact cells of *Rhodobacter capsulatus*. *Biochim. Biophys. Acta.* 975:34–43.

Jones, M. R., and J. B. Jackson. 1990. Proton efflux from right-side-out membrane vesicles of *Rhodobacter sphaeroides* after short flashes. *Biochim. Biophys. Acta.* 1019:51–58.

Junge, W. 1987. Complete tracking of transient proton flow through active chloroplast ATP synthase. *Proc. Natl. Acad. Sci. USA.* 84:7084–7088.

Junge, W., A. McGeer, and W. Ausländer. 1978. Calibration of flash induced pH changes inside thylakoids and kinetic resolution of proton ejection and consumption. *In* Frontiers of Biological Energetics, Vol. 1. P. L. Dutton, J. S. Leigh, J. S. Scarpa, editors. Academic Press, New York. 275–283.

Junge, W., and S. McLaughlin. 1987. The role of fixed and mobile buffers in the kinetics of proton movement. *Biochim. Biophys. Acta.* 890:1–5.

Junge, W., and A. Polle. 1986. Theory of proton flow along appressed thylakoid membranes under both non-stationary and stationary conditions. *Biochim. Biophys. Acta.* 848:265–273.

Kano, K., and J. H. Fendler. 1978. Pyranine as a sensitive pH probe for liposome interiors and surfaces. pH gradients across phospholipid vesicles. *Biochim. Biophys. Acta.* 509:289–299.

Kell, D. B. 1979. On the functional proton current pathway of electron transport phosphorylation. An electrodic view. *Biochim. Biophys. Acta.* 549:55–99.

Kotlyar, A. B., N. Borovok, S. Kiryati, E. Nachliel, and M. Gutman. 1994. The dynamics of proton transfer at the C side of the mitochondrial membrane: picosecond and microsecond measurements. *Biochemistry.* 33:873–879.

Krulwich, T. A., M. Ito, R. Gilmour, M. G. Sturr, A. A. Guffanti, and D. B. Hicks. 1996. Energetic problems of extremely alkaliphilic aerobes. *Biochim. Biophys. Acta.* 1275:21–26.

Maroti, P., and C. A. Wraight. 1997. Kinetics of H^+ ion binding by the P^+Q_A-state of bacterial photosynthetic reaction centers: rate limitation within the protein. *Biophys. J.* 73:367–381.

Michel, H., and D. Oesterhelt. 1980. Electrochemical proton gradient across the cell membrane of *Halobacterium halobium*: comparison of the light-induced increase with the increase of intracellular adenosine triphosphate under steady-state illumination. *Biochemistry.* 19:4615–4619.

Mitchell, P. 1961. Coupling of photophosphorylation to electron and hydrogen transfer by a chemiosmotic type of mechanism. *Nature.* 191: 144–148.

Mulkidjanian, A. Y., and W. Junge. 1994. Calibration and time resolution of lumenal pH-transients in chromatophores of Rhodobacter capsulatus following a single turnover flash of light: proton release by the cytochrome bc_1-complex is strongly electrogenic. *FEBS Lett.* 353:189–193.

Nachliel, E., and M. Gutman. 1996. Quantitative evaluation of the dynamics of proton transfer from photoactivated bacteriorhodopsin to the bulk. *FEBS Lett.* 393:221–225.

Nachliel, E., M. Gutman, S. Kiryati, and N. A. Dencher. 1996. Protonation dynamics of the extracellular and cytoplasmic surface of bacteriorhodopsin in the purple membrane. *Proc. Natl. Acad. Sci. USA.* 93:10747–10752.

Okamura, M. Y., M. L. Paddock, M. S. Graige, and G. Feher. 2000. Proton and electron transfer in bacterial reaction centers. *Biochim. Biophys. Acta.* 1458:148–163.

Packham, N. K., J. A. Berriman, and J. B. Jackson. 1978. The charging capacitance of the chromatophore membrane. *FEBS Lett.* 89:205–210.

Polle, A., and W. Junge. 1989. Proton diffusion along the membrane surface of thylakoids is not enhanced over that in bulk water. *Biophys. J.* 56:27–31.

Porschke, D. 2002. Reaction coupling, acceptor pK, and diffusion control in light induced proton release of bacteriorhodopsin. *J. Phys. Chem. B.* 106:10233–10241.

Schatzler, B., N. A. Dencher, J. Tittor, D. Oesterhelt, S. Yaniv-Checover, E. Nachliel, and M. Gutman. 2003. Subsecond proton-hole propagation in bacteriorhodopsin. *Biophys. J.* 84:671–686.

Scherrer, P., U. Alexiev, T. Marti, H. G. Khorana, and M. P. Heyn. 1994. Covalently bound pH-indicator dyes at selected extracellular or cytoplasmic sites in bacteriorhodopsin. 1. Proton migration along the surface of bacteriorhodopsin micelles and its delayed transfer from surface to bulk. *Biochemistry.* 33:13684–13692.

Sedgwick, E. G., and P. D. Bragg. 1990. pH probes respond to redox changes in cytochrome *o*. *Arch. Biochem. Biophys.* 282:372–376.

Serowy, S., S. M. Saparov, Y. N. Antonenko, W. Kozlovsky, V. Hagen, and P. Pohl. 2003. Structural proton diffusion along lipid bilayers. *Biophys. J.* 84:1031–1037.

Talkner, P. 1995. Anharmonic barrier corrections for the Kramers rate problem in the spatial diffusion regime. *In* New Trends in Kramers Reaction Rate Theory. P. Talkner and P. Hänggi, editors. Kluwer Academic Publishers, Dordrecht, Boston, MA and London, UK. 47–68.

Teschke, O., G. Ceotto, and E. F. de Souza. 2001. Interfacial water dielectric-permittivity-profile measurements using atomic force microscopy. *Phys. Rev. E.* 64:011605.

Varela, L. M., M. Garcia, and V. Mosquera. 2003. Exact mean-field theory of ionic solutions: non-Debye screening. *Physics Reports-Review Section of Physics Letters.* 382:1–111.

Williams, R. J. 2001. The structures of organelles and reticula: localised bioenergetics and metabolism. *Chembiochem.* 2:637–641.

Williams, R. J. 1978. The multifarious couplings of energy transduction. *Biochim. Biophys. Acta.* 505:1–44.

Yam, R., E. Nachliel, S. Kiryati, M. Gutman, and D. Huppert. 1991. Proton transfer dynamics in the nonhomogeneous electric field of a protein. *Biophys. J.* 59:4–11.

Zhang, J., and P. R. Unwin. 2002. Proton diffusion at phospholipid assemblies. *J. Am. Chem. Soc.* 124:2379–2383.

Ziegler, M., and H. S. Penefsky. 1993. The adenine nucleotide translocase modulates oligomycin-induced quenching of pyranine fluorescence in submitochondrial particles. *J. Biol. Chem.* 268:25320–25328.